

Probing dark matter self-interaction in the Sun with IceCube-PINGU

Chian-Shu Chen,^{a,c} Fei-Fan Lee,^b Guey-Lin Lin^b and Yen-Hsun Lin^b

^aPhysics Division, National Center for Theoretical Sciences,
Hsinchu 30010, Taiwan

^bInstitute of Physics, National Chiao Tung University,
Hsinchu 30010, Taiwan

^cDepartment of Physics, National Tsing Hua University,
Hsinchu 30010, Taiwan

E-mail: chianshu@phys.sinica.edu.tw, fflee@mail.nctu.edu.tw, glin@cc.nctu.edu.tw,
chris.py99g@g2.nctu.edu.tw

Received September 12, 2014

Accepted October 1, 2014

Published October 20, 2014

Abstract. We study the capture, annihilation and evaporation of dark matter (DM) inside the Sun. It has been shown that the DM self-interaction can increase the DM number inside the Sun. We demonstrate that this enhancement becomes more significant in the regime of small DM mass, given a fixed DM self-interaction cross section. This leads to the enhancement of neutrino flux from DM annihilation. On the other hand, for DM mass as low as a few GeVs, not only the DM-nuclei scatterings can cause the DM evaporation, DM self-interaction also provides non-negligible contributions to this effect. Consequently, the critical mass for DM evaporation (typically 3 ~ 4 GeV without the DM self-interaction) can be slightly increased. We discuss the prospect of detecting DM self-interaction in IceCube-PINGU using the annihilation channels $\chi\chi \rightarrow \tau^+\tau^-$, $\nu\bar{\nu}$ as examples. The PINGU sensitivities to DM self-interaction cross section $\sigma_{\chi\chi}$ are estimated for track and cascade events.

Keywords: dark matter theory, neutrino detectors

ArXiv ePrint: [1408.5471](https://arxiv.org/abs/1408.5471)



Contents

1	Introduction	1
2	DM accumulation in the Sun	2
2.1	DM evolution equation	2
2.2	Numerical results	5
3	Probing DM self-interaction at IceCube-PINGU	8
4	Conclusion	12
A	DM self-interaction induced evaporation	12

1 Introduction

Convincing observational evidences indicate that roughly 80% of the matter in our universe is dark matter (DM). On the other hand, the understanding of the DM nature is still at the budding stage. If the form of DM is any kind of elementary particle χ , theoretical predictions for its mass lie in a wide range, from sub-eV scale to grand unified scale. Even though, more and more experimental searches, including direct and indirect detection with terrestrial or satellite instruments, are looking for the DM signals. The knowledge on DM is accumulating rapidly. If DM interacts with ordinary matters weakly, it may leave tracks in the detector and be caught directly. The possibility to see such signals depends on DM mass and its interaction cross section with the ordinary matter in the detector. The situation is similar for the indirect searches where one looks for the flux excess in cosmic rays, gamma rays, and neutrinos. The flux excess for the above particles are due to DM annihilation or DM decays. Different search strategies would have sensitivities to different parameter ranges and all together cover quite a broad range for DM mass and DM interaction cross section, respectively.

In this paper, we study the general framework of DM capture, annihilation and evaporation in the Sun. The capture of galactic DM by the Sun through DM-nuclei collisions was first proposed and calculated in refs. [1–7]. It was then observed that the assumption of DM thermal distribution according to the average temperature of the Sun is a good approximation for capture and annihilation processes, but the correction to the evaporation mass can reach to 8% in the true distribution calculation [8]. The abundance of DM inside the Sun hence results from the balancing among DM capture, annihilation and evaporation processes. Updated calculations on these processes are given in refs. [9–11].

In our study, we particularly note that for both collisionless cold DM and warm DM there exists a so-called core/cusp problem [12] which addresses the discrepancy between the computational structure simulation and the actual observation [13–18]. DM self-interaction has been introduced to resolve this inconsistency [19]. This type of analyses put constraints on the ratio of DM self-interaction cross section to the DM mass, $0.1 < \sigma_{\chi\chi}/m_\chi < 1.0$ (cm²/g), from observations of various galactic structures [20–23]. It is worth mentioning that the authors in ref. [24] used the IceCube data [25] to constrain the magnitude of $\sigma_{\chi\chi}$ for m_χ in the range of $\mathcal{O}(10)$ GeV to $\mathcal{O}(1)$ TeV (also see the study of high energy neutrino flux from

DM annihilation within the Sun with the inclusion of DM self-interaction in ref. [26]). In their work the evaporation effect can be neglected for the considered DM mass region and the detectability of $\sigma_{\chi\chi}$ by the IceCube through observing the final state neutrino flux produced by the DM annihilation is analyzed. In this paper we shall concentrate on the low mass region of $\mathcal{O}(1)$ GeV DM mass since such a mass range has not been probed by the IceCube data mentioned above. Furthermore, this is also the mass range where the indirect search is crucial. In the case of spin-independent interaction, the sensitivity of DM direct search quickly turns poor for m_χ less than 10 GeV [27]. Therefore the IceCube-PINGU [28] detector with a 1 GeV threshold energy could be more sensitive than some of the direct detection experiments for $m_\chi < 10$ GeV. For spin-dependent interaction, the IceCube-PINGU sensitivity has been estimated to be much better than constraints set by direct detection experiments [29].

For illustrative purpose, we shall only consider neutrino flux produced by DM annihilating into leptons such as $\chi\chi \rightarrow \tau^+\tau^-$ and $\chi\chi \rightarrow \nu\bar{\nu}$, respectively. The final-state neutrinos can be detected by terrestrial neutrino telescopes such as IceCube-PINGU [28]. We do not consider $\chi\chi \rightarrow \mu^+\mu^-$ because muons will suffer severe energy losses in the Sun before they decay to neutrinos. The soft neutrino spectrum in this case is dominated by the atmospheric background. One also expects that the neutrino telescopes are less sensitive to heavy quark channels such as $\chi\chi \rightarrow b\bar{b}$ than their sensitivities to leptonic channels. This is caused by the relatively softer neutrino spectrum resulting from the b -hadron decays compared to the neutrino spectrum from τ decays [30]. For light quark channels $\chi\chi \rightarrow q\bar{q}$, the hadronic cascades produce pions or kaons in large multiplicities. These hadrons decay almost at rest and produce MeV neutrino fluxes, which from the observational point of view could be as promising as the hard spectrum channels [10, 31]. However we would not discuss these signatures because the threshold energy of IceCube-PINGU is in the GeV range.

For $\mathcal{O}(1)$ GeV DM mass, it is necessary to consider evaporation processes for determining the DM abundance inside the Sun. We shall demonstrate that DM evaporation can arise both from DM-nuclei scatterings and DM self-interactions. In fact the inclusion of DM self-interaction can raise the critical mass such that evaporation can take place for DM lighter than this mass scale. On the other hand, DM self-interaction also enhances total DM number trapped inside the Sun for m_χ greater than the critical mass.

This paper is organized as follows. In section II, we calculate the DM number accumulated inside the Sun via four processes. We then present the parameter space in which the equilibrium condition holds. In section III, we present the numerical results of our analysis. The sensitivity of IceCube-PINGU to DM self-interaction inside the Sun is presented in section IV. Finally, we conclude in section V.

2 DM accumulation in the Sun

2.1 DM evolution equation

We assume that both the galactic DM and the nuclei inside the Sun follow the thermal distributions. If DM interacts with nuclei in the Sun then it can be captured by the Sun when its final velocity is smaller than the escape velocity from the Sun. Alternatively, DM trapped inside the Sun will be kicked out if its final velocity after the scattering with the nuclei is larger than the escape velocity. The inclusion of DM self-interaction will also have effects on the capture and evaporation of DM inside the Sun. We will come to details of this in the later discussion. The captured DM could have reached to an equilibrium state if the equilibrium time scale is less than the age of the Sun ($t_\odot \approx 10^{17}s$). The general DM

evolution equation in the Sun is given by

$$\frac{dN_\chi}{dt} = C_c + (C_s - C_e)N_\chi - (C_a + C_{se})N_\chi^2 \quad (2.1)$$

with N_χ the DM number in the Sun, C_c the rate at which DM are captured by the Sun, C_s the rate at which DM are captured due to their scattering with DM that have already been trapped in the Sun, C_e the the DM evaporation rate due to DM-nuclei interactions, C_a the DM annihilation rate, and C_{se} the evaporation rate induced by the interaction between DM particles in the Sun. The coefficients $C_{a,c,e,s,se}$ are taken to be positive and *time-independent*.

We note that C_c can be categorized by the type of interactions between DM particles and nucleons. For spin-dependent (SD) interactions, the capture rate is given by [6, 7]

$$C_c^{\text{SD}} \simeq 3.35 \times 10^{24} \text{ s}^{-1} \left(\frac{\rho_0}{0.3 \text{ GeV/cm}^3} \right) \left(\frac{270 \text{ km/s}}{\bar{v}} \right)^3 \left(\frac{\text{GeV}}{m_\chi} \right)^2 \left(\frac{\sigma_{\text{H}}^{\text{SD}}}{10^{-6} \text{ pb}} \right), \quad (2.2)$$

where ρ_0 is the local DM density, \bar{v} is the velocity dispersion, $\sigma_{\text{H}}^{\text{SD}}$ is the SD DM-hydrogen scattering cross section and m_χ is the DM mass. The capture rate from spin-independent (SI) scattering is given by [6, 7]

$$C_c^{\text{SI}} \simeq 1.24 \times 10^{24} \text{ s}^{-1} \left(\frac{\rho_0}{0.3 \text{ GeV/cm}^3} \right) \left(\frac{270 \text{ km/s}}{\bar{v}} \right)^3 \left(\frac{\text{GeV}}{m_\chi} \right)^2 \left(\frac{2.6\sigma_{\text{H}}^{\text{SI}} + 0.175\sigma_{\text{He}}^{\text{SI}}}{10^{-6} \text{ pb}} \right). \quad (2.3)$$

Here $\sigma_{\text{H}}^{\text{SI}}$ and $\sigma_{\text{He}}^{\text{SI}}$ are SI DM-hydrogen and -helium cross sections respectively. Taking the approximation $m_p \approx m_n$, the DM-nucleus cross section σ_i is related to DM-nucleon cross section $\sigma_{\chi p}$ by

$$\sigma_i^{\text{SD}} = A^2 \left(\frac{m_\chi + m_p}{m_\chi + m_A} \right)^2 \frac{4(J_i + 1)}{3J_i} |\langle S_{p,i} \rangle + \langle S_{n,i} \rangle|^2 \sigma_{\chi p}^{\text{SD}} \quad (2.4)$$

for SD interactions and

$$\sigma_i^{\text{SI}} = A^2 \left(\frac{m_A}{m_p} \right)^2 \left(\frac{m_\chi + m_p}{m_\chi + m_A} \right)^2 \sigma_{\chi p}^{\text{SI}} \quad (2.5)$$

for SI interactions, where A is the atomic number, m_A the mass of the nucleus, J_i the total angular momentum of the nucleus and $\langle S_{p,i} \rangle$ and $\langle S_{n,i} \rangle$ the spin expectation values of proton and of neutron averaged over the entire nucleus [32–35].

The DM evaporation rate in the Sun, C_e , has been well investigated in refs. [5, 8]. The evaporation rate is usually ignored in the DM evolution equation since it happens for a very low DM mass, $m_\chi \lesssim 3 \text{ GeV}$. A updated calculation in ref. [11] has shown that, for $m_\chi/m_A > 1$,

$$C_e \simeq \frac{8}{\pi^3} \sqrt{\frac{2m_\chi}{\pi T_\chi(\bar{r})}} \frac{v_{\text{esc}}^2(0)}{\bar{r}^3} \exp \left(-\frac{m_\chi v_{\text{esc}}^2(0)}{2T_\chi(\bar{r})} \right) \Sigma_{\text{evap}}, \quad (2.6)$$

where $v_{\text{esc}}(0)$ is the escape velocity from the core of the Sun, T_χ is the DM temperature in the Sun, and \bar{r} is average DM orbit radius which is the mean DM distance from the solar center. The quantity Σ_{evap} is the sum of the scattering cross sections of all the nuclei within a radius $r_{95\%}$, where the solar temperature has dropped to 95% of the DM temperature. Although the approximate form of C_e can be obtained as the above equation, we shall adopt the exact form of C_e given in ref. [8] for our subsequent numerical calculations.

As stated before, C_s is the DM capture rate by scattering off the DM that have been captured inside the Sun. This kind of scattering may result in the target dark matter particles being ejected from the Sun upon recoil. However, because the escape speed from the Sun is sufficiently large, the effect of target DM ejection by recoil is only a small correction to the simple solar capture estimate. Hence the self-capture rate in the Sun can be approximated by [26]

$$C_s = \sqrt{\frac{3}{2}} n_\chi \sigma_{\chi\chi} v_{\text{esc}}(R_\odot) \frac{v_{\text{esc}}(R_\odot)}{\bar{v}} \langle \hat{\phi}_\chi \rangle \frac{\text{erf}(\eta)}{\eta}, \quad (2.7)$$

where $\langle \hat{\phi}_\chi \rangle \simeq 5.1$ [36] is a dimensionless average solar potential experienced by the captured DM within the Sun, n_χ is the local number density of halo DM, $\sigma_{\chi\chi}$ is the elastic scattering cross section of DM with themselves, $v_{\text{esc}}(R_\odot)$ is the Sun's escape velocity at the surface, and $\eta^2 = 3(v_\odot/\bar{v})^2/2$ is the square of a dimensionless velocity of the Sun through the Galactic halo with $v_\odot = 220$ km/s Sun's velocity and $\bar{v} = 270$ km/s the local velocity dispersion of DM in the halo.

C_a is the annihilation coefficient given by [5]

$$C_a \simeq \frac{\langle \sigma v \rangle V_2}{V_1^2}, \quad (2.8)$$

where

$$V_j \simeq 6.5 \times 10^{28} \text{ cm}^3 \left(\frac{10 \text{ GeV}}{jm_\chi} \right)^{3/2} \quad (2.9)$$

is the DM effective volume inside the Sun and $\langle \sigma v \rangle$ is the relative velocity averaged annihilation cross section.

C_{se} is the self-interaction induced evaporation. Since the DM can interact among themselves, DM trapped in the solar core could scatter with other trapped DM and results in the evaporation. Essentially, one of the DM particles could have velocity greater than the escape velocity after the scattering. This process involves two DM particles just like annihilation. We note that both processes lead to the DM dissipation in the Sun. On the other hand C_{se} does not produce neutrino flux as C_a does. Since the derivation of C_{se} has not been given in the previous literature, we present some details of the derivation in appendix A.¹

With $N_\chi(0) = 0$ as the initial condition, the general solution to eq. (2.1) is

$$N_\chi(t) = \frac{C_c \tanh(t/\tau_A)}{\tau_A^{-1} - (C_s - C_e) \tanh(t/\tau_A)/2}, \quad (2.10)$$

with

$$\tau_A = \frac{1}{\sqrt{C_c(C_a + C_{se}) + (C_s - C_e)^2/4}} \quad (2.11)$$

the time-scale for the DM number in the Sun to reach the equilibrium. If the equilibrium state is achieved, i.e., $\tanh(t/\tau_A) \sim 1$, one has

$$N_{\chi,\text{eq}} = \frac{C_s - C_e}{2(C_a + C_{se})} + \sqrt{\frac{(C_s - C_e)^2}{4(C_a + C_{se})^2} + \frac{C_c}{C_a + C_{se}}}. \quad (2.12)$$

¹We thank S. Palomares-Ruiz for pointing out to us the importance of C_{se} .

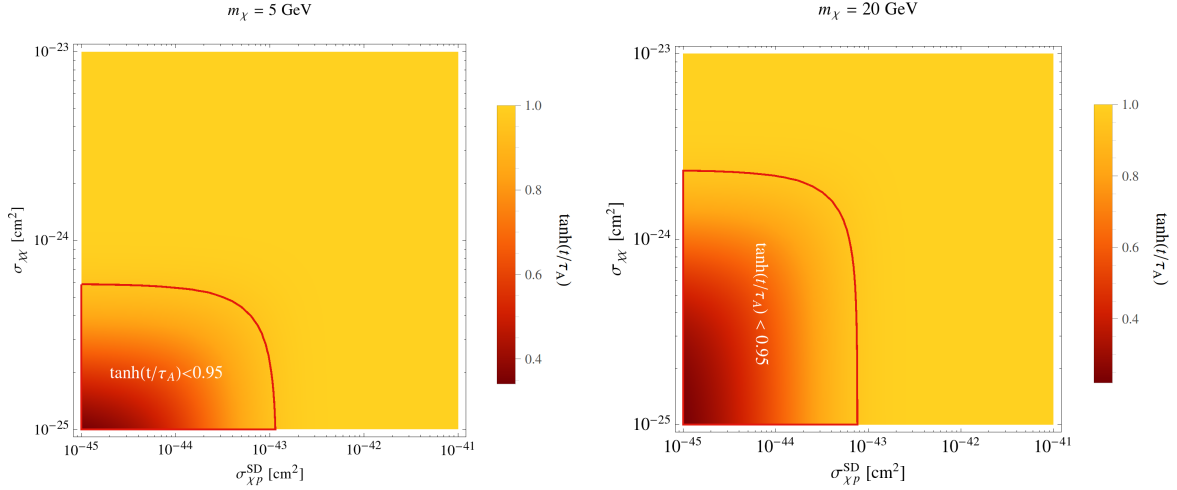


Figure 1. The values of $\tanh(t/\tau_A)$ over $\sigma_{\chi p}^{\text{SD}} - \sigma_{\chi\chi}$ plane at the present day, $t = t_\odot$. The red-circled area is the non-equilibrium region for N_χ .

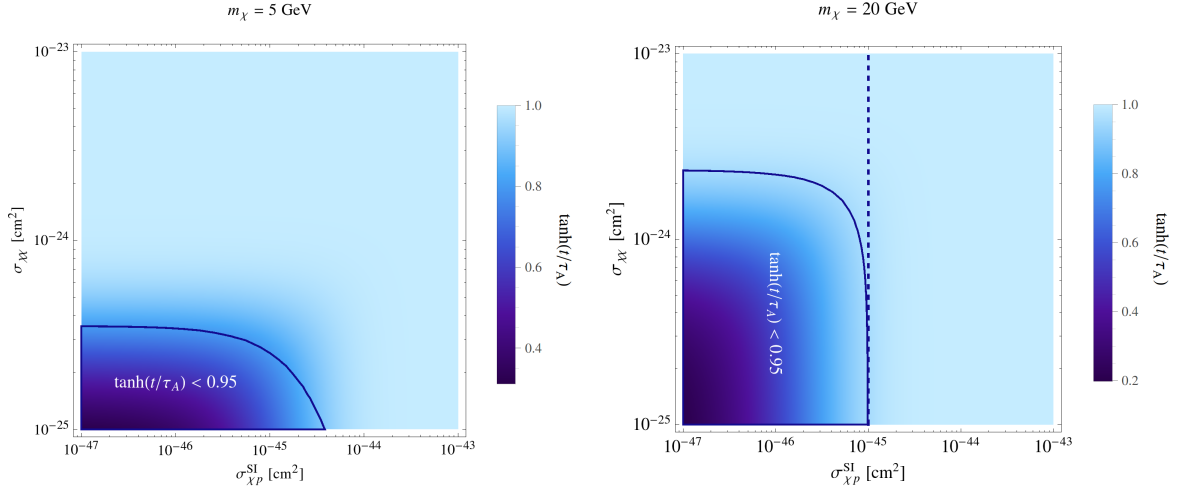


Figure 2. The values of $\tanh(t/\tau_A)$ over $\sigma_{\chi p}^{\text{SI}} - \sigma_{\chi\chi}$ plane at the present day, $t = t_\odot$. The blue-circled area is the non-equilibrium region for N_χ . The vertical line at the right panel indicates the LUX bound, $\sigma_{\chi p}^{\text{SI}} \leq 10^{-45} \text{ cm}^2$, for $m_\chi = 20 \text{ GeV}$.

The DM annihilation rate in the Sun's core is given by

$$\Gamma_A = \frac{C_a}{2} N_\chi^2. \quad (2.13)$$

By setting $C_s = C_{se} = 0$, we can recover the results in refs. [5, 8–11] for the absence of DM self-interaction. By setting $C_e = C_{se} = 0$, we recover the result in ref. [26], which includes the DM self-interaction while neglects the DM evaporation.

2.2 Numerical results

The coefficients $C_{c,e,s}$ have been worked out in refs. [5, 8, 26], which we adopt for our numerical studies. The numerical result for C_{se} is based on the analytic expression we have given in

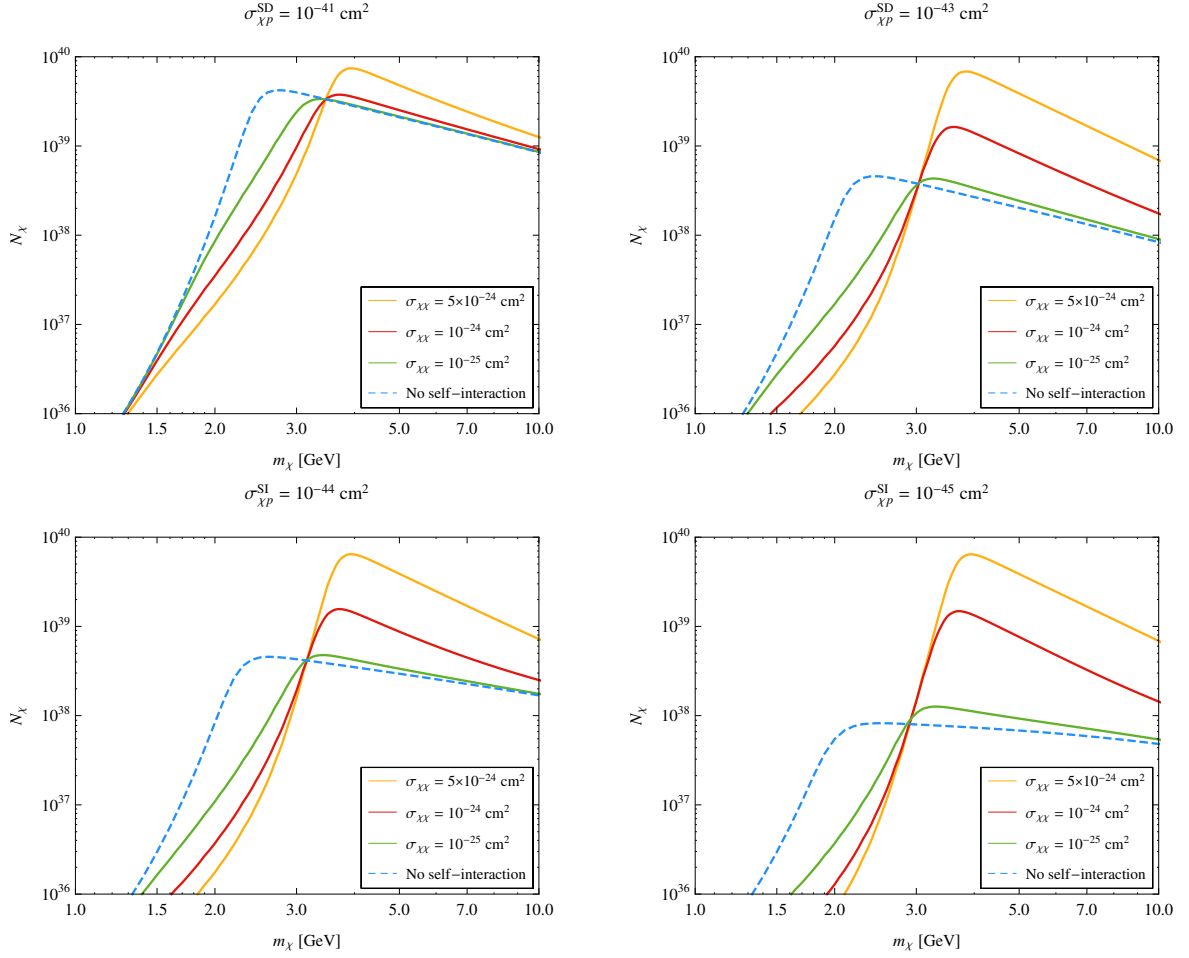


Figure 3. The number of DM particles trapped inside the Sun, N_χ , as a function of DM mass m_χ with and without DM self-interaction. Both SI and SD DM-nucleon couplings are considered. Different colors represent different values for $\sigma_{\chi\chi}$. The peak for each parameter set is the maximal DM number trapped inside the Sun, and the corresponding DM mass can be viewed as the evaporation mass scale since N_χ drops quickly for m_χ smaller than this mass scale.

the appendix. We first identify the equilibrium region on the $\sigma_{\chi p}$ - $\sigma_{\chi\chi}$ plane. The SD and SI cases are presented in figure 1 and figure 2, respectively with two benchmark DM masses $m_\chi = 5$ GeV and 20 GeV. We have taken $10^{-45} \leq \sigma_{\chi p}^{\text{SD}}/\text{cm}^2 \leq 10^{-41}$ and $10^{-47} \leq \sigma_{\chi p}^{\text{SI}}/\text{cm}^2 \leq 10^{-43}$ for our studies. The range of SD cross section is below those bounds set by direct detection experiments, COUPP [37] and Simple [38], and the indirect search by IceCube [25] for $m_\chi \approx 20$ GeV. This range of SI cross section is below the direct detection bound set by LUX [39] at $m_\chi = 5$ GeV. For $m_\chi = 20$ GeV, the LUX bound on $\sigma_{\chi p}^{\text{SI}}$ is 10^{-45} cm^2 . We have indicated this bound on the right panel of figure 2. The dark areas represent those regions with $\tanh(t/\tau_A) \lesssim 1$ at the present day whereas the light areas are the equilibrium regions.

In figure 3, we show the effect of DM self-interaction on the number of DM particles trapped inside the Sun. It is seen that N_χ can be significantly enhanced for sufficiently large $\sigma_{\chi\chi}$. The N_χ peak for each parameter set is the maximal DM number trapped inside the Sun, and the corresponding DM mass can be viewed as the evaporation mass scale because N_χ drops quickly for m_χ smaller than this mass scale. We observe that the inclusion of

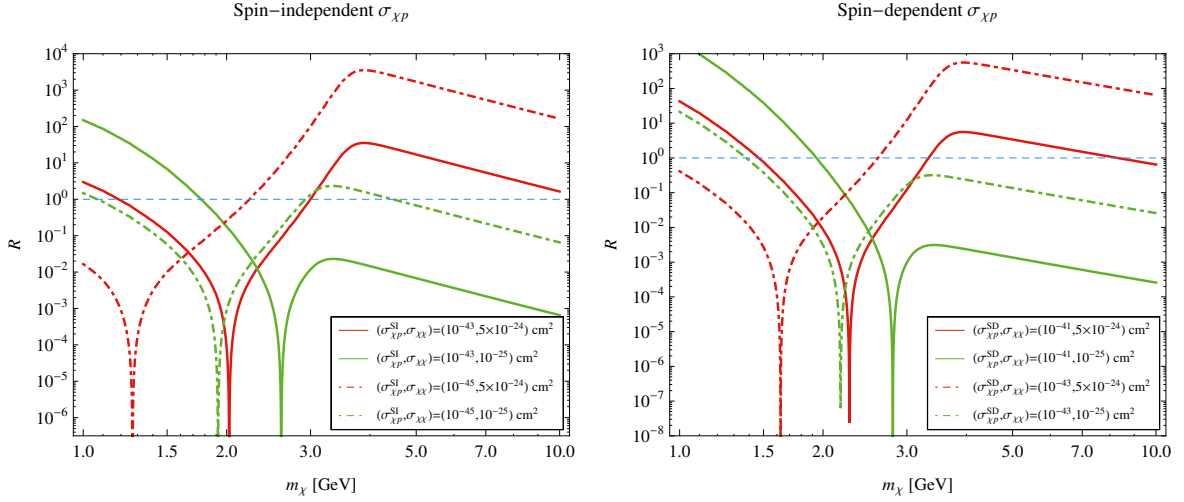


Figure 4. Ratio R versus DM mass m_χ . The dip occurs when DM self-interaction and evaporation effects cancel each other, $C_e \approx C_s$.

DM self-interaction tends to lift the evaporation mass by about 1 GeV. This is because the evaporation due to the captured DM-DM self-interaction comes to operate.

To quantify the effects of DM self-interaction and evaporation (the one by C_e) on N_χ , it is useful to define a dimensionless parameter R by

$$R \equiv \frac{(C_s - C_e)^2}{C_c(C_a + C_{se})}, \quad (2.14)$$

such that

$$N_{\chi,\text{eq}} = \sqrt{\frac{C_c}{C_a + C_{se}}} \left(\pm \sqrt{\frac{R}{4}} + \sqrt{\frac{R}{4} + 1} \right), \quad (2.15)$$

and

$$\Gamma_A = \frac{1}{2} \frac{C_c C_a}{C_a + C_{se}} \left(\pm \sqrt{\frac{R}{4}} + \sqrt{\frac{R}{4} + 1} \right)^2, \quad (2.16)$$

where one takes the positive sign for $C_s > C_e$ and the negative sign for $C_e > C_s$. The expression for N_χ in the non-equilibrium case can also be simplified in a similar way. Comparing C_s with C_e , DM self-interaction dominates in the high mass region whereas the evaporation process takes over in the low mass region. Here we have taken into account both effects and found that the transition between two effects occurs at $\mathcal{O}(1)$ GeV DM mass. In figure 4, we show the behavior of R as a function of m_χ . The dip of R for each parameter set represents the narrow mass range where $C_s \approx C_e$. On the right side of the dip, C_s dominates over C_e while the reverse is true on the left side of the dip.

It is seen that R in the evaporation dominant region is growing up in small m_χ since the velocity of final state χ after the collision can easily be larger than the escape velocity from the Sun in this case. The parameter space for $R > 1$ over the $\sigma_{\chi p} - \sigma_{\chi\chi}$ plane is shown in figure 5 for $m_\chi = 5$ and 20 GeV. Since $C_e < C_s$ for the above chosen m_χ , hence $R > 1$ is the

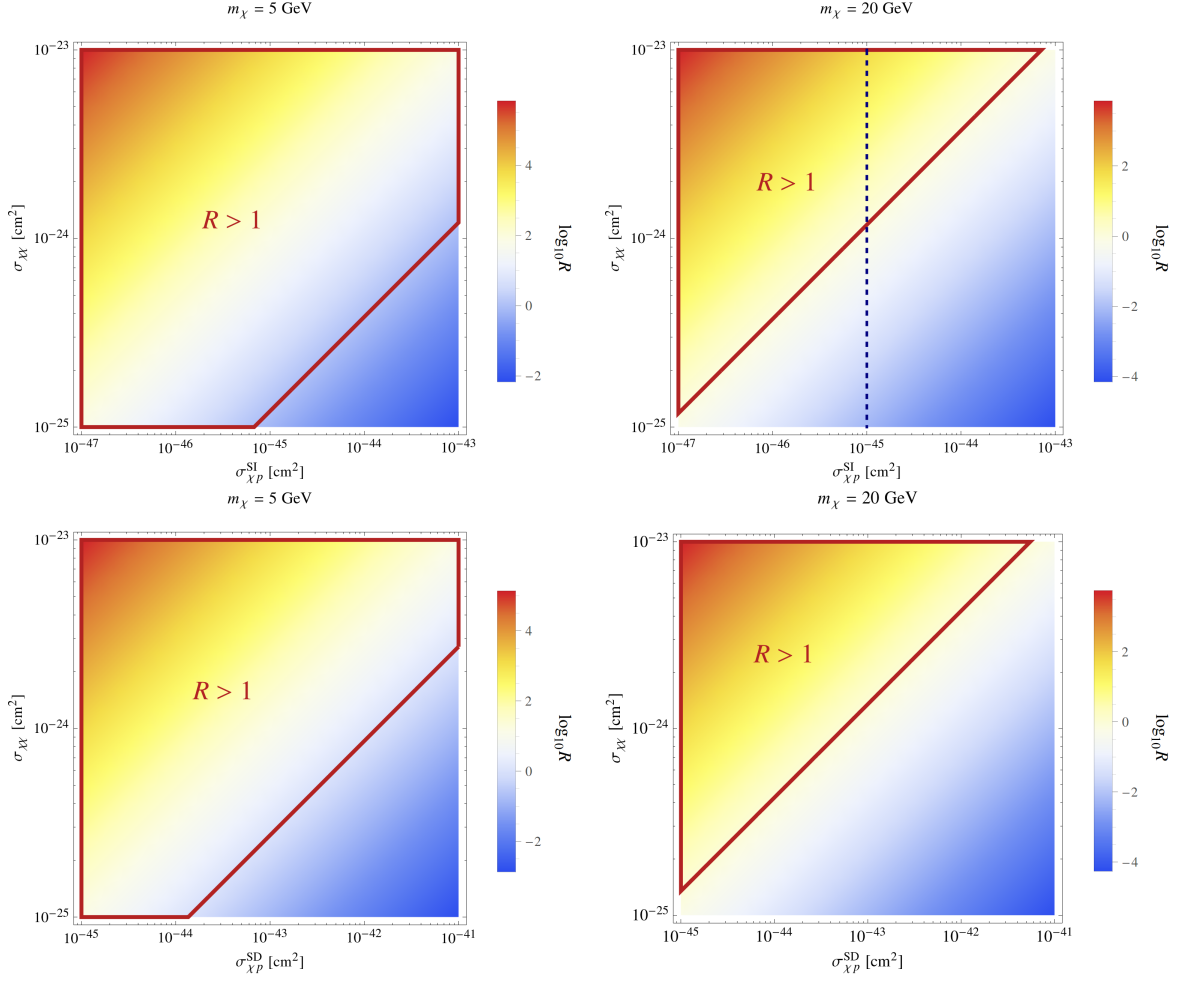


Figure 5. Ratio R over the $\sigma_{\chi p} - \sigma_{\chi\chi}$ plane. The upper panel is for SI interaction and the lower panel is for SD interaction. The red-circled region is for $R > 1$.

region where DM self-interaction is relevant. It has been seen that DM self-interaction not only enhances N_χ significantly for $m_\chi < 10$ GeV but also affects the evaporation mass scale. Therefore in the next session we shall explore the possibility of probing DM self-interaction for $m_\chi < 10$ GeV by IceCube-PINGU detector.

3 Probing DM self-interaction at IceCube-PINGU

The annihilation rate of the captured DM in the Sun is given by eq. (2.13). It is worth mentioning that in the absence of both evaporation (the one due to C_e) and self-interaction, the annihilation rate Γ_A with an equilibrium N_χ is

$$\Gamma_A = \frac{1}{2} C_a \times \frac{C_c}{C_a} = \frac{C_c}{2}, \quad (3.1)$$

which only depends on the capture rate C_c . However, with the presence of either C_e or self-interaction, Γ_A depends on other coefficients as well even N_χ has reached to the equilibrium. We plot Γ_A as a function of m_χ with and without self-interaction in figure 6.

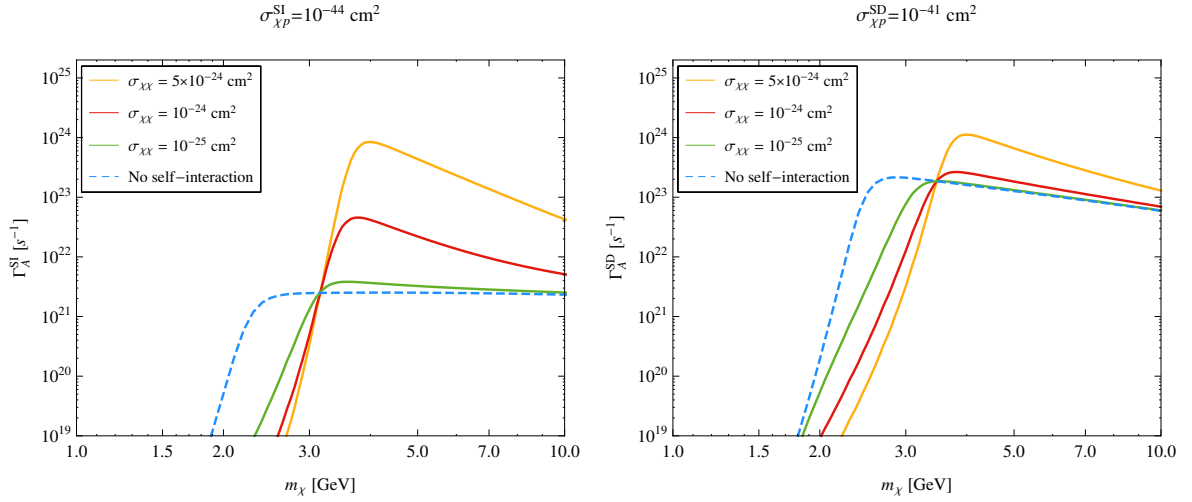


Figure 6. The annihilation rate Γ_A of the captured DM inside the Sun. The left panel assumes DM-nuclei scattering is dominated by SI interaction while the right panel assumes such scattering is dominated by SD interaction.

To probe DM self-interaction for small m_χ , we consider DM annihilation channels, $\chi\chi \rightarrow \tau^+\tau^-$ and $\nu\bar{\nu}$, for producing neutrino final states to be detected by IceCube-PINGU [28]. The neutrino differential flux of flavor i , Φ_{ν_i} , from $\chi\chi \rightarrow f\bar{f}$ can be expressed as

$$\frac{d\Phi_{\nu_i}}{dE_{\nu_i}} = P_{\nu_j \rightarrow \nu_i}(E_\nu) \frac{\Gamma_A}{4\pi R_\odot^2} \sum_f B_f \left(\frac{dN_{\nu_j}}{dE_{\nu_j}} \right) \quad (3.2)$$

where R_\odot is the distance between the neutrino source and the detector, $P_{\nu_j \rightarrow \nu_i}(E_\nu)$ is the neutrino oscillation probability during the propagation, B_f is the branching ratio corresponding to the channel $\chi\chi \rightarrow f\bar{f}$, dN_ν/dE_ν is the neutrino spectrum at the source, and Γ_A is the DM annihilation rate in the Sun. To compute dN_ν/dE_ν , we employed WimpSim [40] with a total of 50,000 Monte-Carlo generated events.

The neutrino event rate in the detector is given by

$$N_\nu = \int_{E_{\text{th}}}^{m_\chi} \frac{d\Phi_\nu}{dE_\nu} A_\nu(E_\nu) dE_\nu d\Omega \quad (3.3)$$

where E_{th} is the detector threshold energy, $d\Phi_\nu/dE_\nu$ is the neutrino flux from DM annihilation, A_ν is the detector effective area, and Ω is the solid angle. We study both muon track events and cascade events induced by neutrinos. The PINGU module will be implanted inside the IceCube in the near future [28] and can be used to probe neutrino energy down to $\mathcal{O}(1)$ GeVs. We take ice as the detector medium, so that the IceCube-PINGU neutrino effective area is expressed as

$$A_{\text{eff}}^\nu(E_\nu) = V_{\text{eff}} \frac{N_A}{M_{\text{ice}}} (n_p \sigma_{\nu p}(E_\nu) + n_n \sigma_{\nu n}(E_\nu)), \quad (3.4)$$

where V_{eff} is the IceCube-PINGU effective volume, N_A is the Avogadro constant, M_{ice} is the mass of ice per mole, $n_{p,n}$ is the number of proton/neutron of an ice molecule and $\sigma_{\nu p,n}$ is

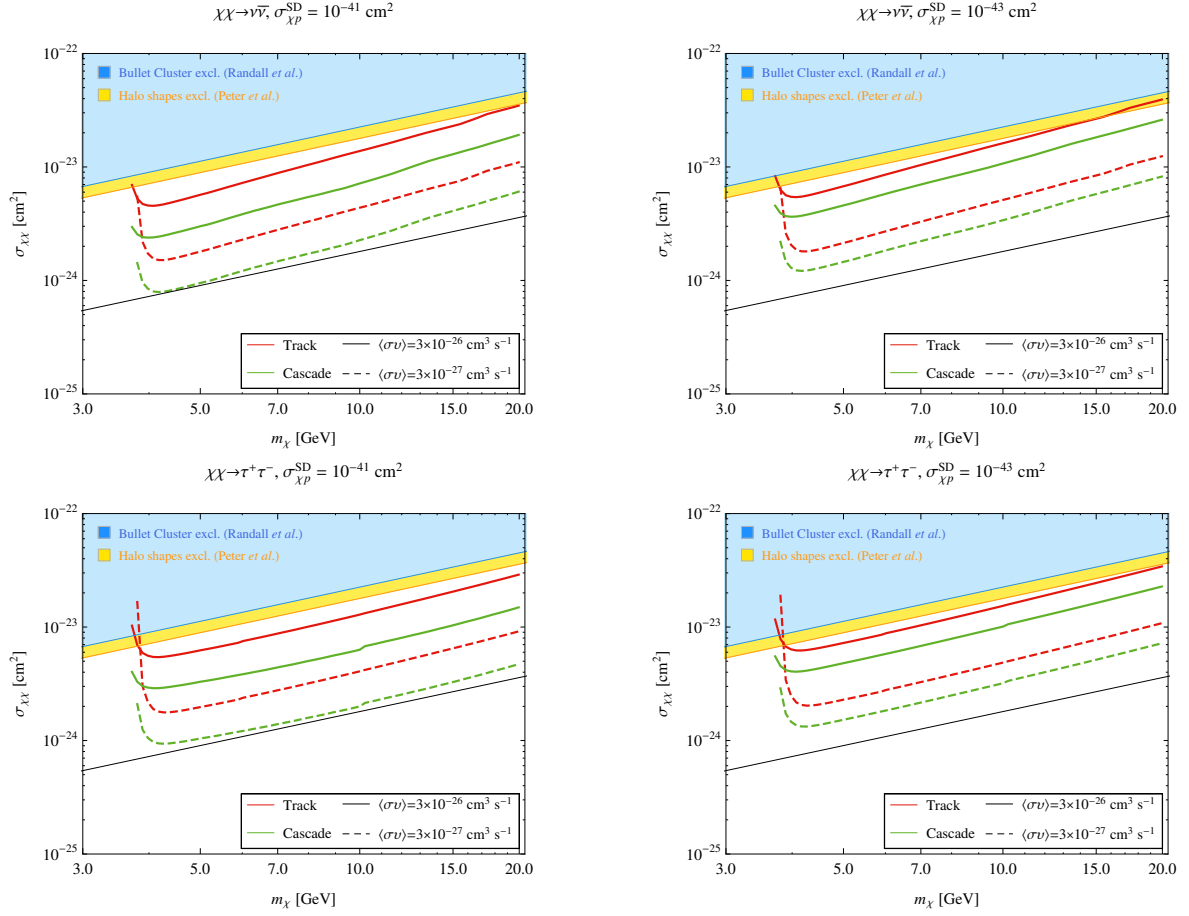


Figure 7. The IceCube-PINGU sensitivities to DM self-interaction cross section $\sigma_{\chi\chi}$ as a function of m_χ . The DM-nucleus interaction inside the Sun is assumed to be dominated by SD interaction.

the neutrino-proton/neutron cross section which can be approximated by [41–44]

$$\frac{\sigma_{\nu N}(E_\nu)}{E_\nu} = 6.66 \times 10^{-3} \text{ pb} \cdot \text{GeV}^{-1}, \quad (3.5a)$$

$$\frac{\sigma_{\bar{\nu} N}(E_\nu)}{E_\nu} = 3.25 \times 10^{-3} \text{ pb} \cdot \text{GeV}^{-1}, \quad (3.5b)$$

for $1 \text{ GeV} \leq E_\nu \leq 10 \text{ GeV}$. As the neutrinos propagate from the source to the detector, they encounter high-density medium in the Sun, the vacuum in space, and the Earth medium. The matter effect to the neutrino oscillation has been considered in $P_{\nu_j \rightarrow \nu_i}$ in eq. (3.2).

The atmospheric background event rate can also be calculated by eq. (3.3) with $d\Phi_\nu/dE_\nu$ replaced by the atmospheric neutrino flux. Hence

$$N_{\text{atm}} = \int_{E_{\text{th}}}^{E_{\text{max}}} \frac{d\Phi_\nu^{\text{atm}}}{dE_\nu} A_\nu(E_\nu) dE_\nu d\Omega. \quad (3.6)$$

In our calculation, the atmospheric neutrino flux $d\Phi_\nu^{\text{atm}}/dE_\nu$ is taken from ref. [45, 46]. We set $E_{\text{max}} = m_\chi$ in order to compare with the DM signal.

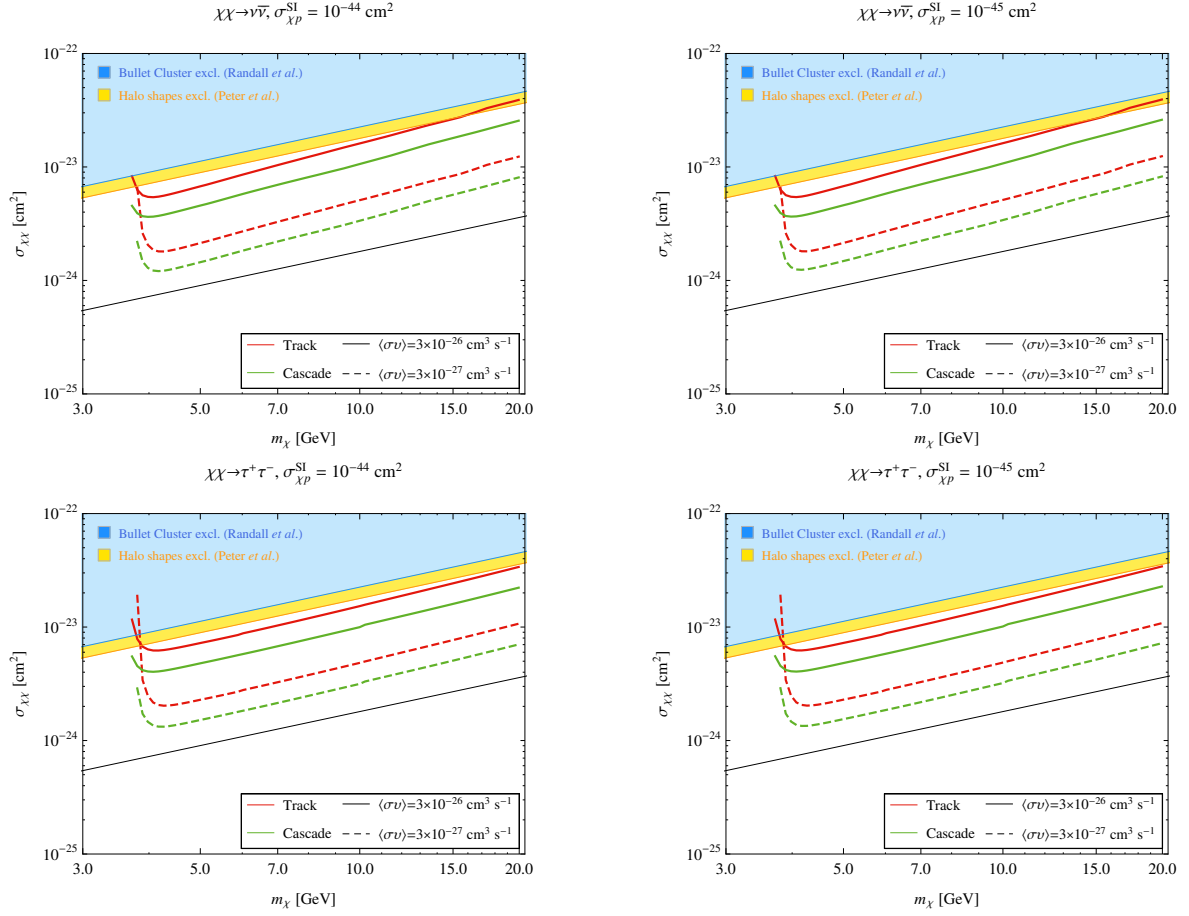


Figure 8. The IceCube-PINGU sensitivities to DM self-interaction cross section $\sigma_{\chi\chi}$ as a function of m_χ . The DM-nucleus interaction inside the Sun is assumed to be dominated by SI interaction.

The angular resolution for IceCube-PINGU detector at $E_\nu = 5$ GeV is roughly 10° [28]. Hence we consider neutrino events arriving from the solid angle range $\Delta\Omega = 2\pi(1 - \cos\psi)$ surrounding the Sun with $\psi = 10^\circ$. We present the IceCube-PINGU sensitivity to $\sigma_{\chi\chi}$ in the DM mass region $3 \text{ GeV} < m_\chi < 20 \text{ GeV}$ for both SD and SI cases in figure 7 and figure 8, respectively. The sensitivities to $\sigma_{\chi\chi}$ are taken to be 2σ significance for 5 years of data taking. The shadow areas in the figures represent those parameter spaces disfavored by the Bullet Cluster and halo shape analyses. Below the black solid line, the DM self-interaction is too weak to resolve the core/cusp problem of the structure formation. Two benchmark values of thermal average cross section, $\langle\sigma v\rangle = 3 \times 10^{-26} \text{ cm}^3 \text{ s}^{-1}$ and $\langle\sigma v\rangle = 3 \times 10^{-27} \text{ cm}^3 \text{ s}^{-1}$ are used for our studies. We note that the latter value for $\langle\sigma v\rangle$ does not contradict with the relic density, since DM annihilation inside the Sun occurs much later than the period of freeze-out.

We take $\sigma_{\chi p}^{\text{SD}} = 10^{-41} \text{ cm}^2$ and 10^{-43} cm^2 for SD interaction, and take $\sigma_{\chi p}^{\text{SI}} = 10^{-44} \text{ cm}^2$ and 10^{-45} cm^2 for SI interaction. We stress that $\sigma_{\chi p}^{\text{SD}} = 10^{-41} \text{ cm}^2$ is below the lowest value of IceCube bound $\sigma_{\chi p}^{\text{SD}} \sim 10^{-40} \text{ cm}^2$ at $m_\chi \sim 300 \text{ GeV}$ [25]. For SI interaction, $\sigma_{\chi p}^{\text{SI}} = 10^{-44} \text{ cm}^2$ is below the LUX bound for $m_\chi < 8 \text{ GeV}$, while $\sigma_{\chi p}^{\text{SI}} = 10^{-45} \text{ cm}^2$ is below the LUX bound for $m_\chi < 20 \text{ GeV}$ [39]. We find that cascade events provide better sensitivities to DM self-interaction than track events do in all cases. One can also see that the sensitivity to $\sigma_{\chi\chi}$

becomes better for smaller annihilation cross section $\langle\sigma v\rangle$ for a fixed $\sigma_{\chi p}$, as noted in earlier works [24, 26] which neglect both C_e and C_{se} . This is evident from eq. (2.16) since R increases as C_a decreases. It is instructive to take the limit $R \gg 1$ such that $\Gamma_A \rightarrow (C_c C_a)R/2(C_a + C_{se})$ for $C_s > C_e$. It is easily seen that Γ_A is inversely proportional to C_a (in the mass range that C_{se} is negligible) and is independent of C_e . In other words, only C_s and C_a determine the annihilation rate (we are in the region that C_e is suppressed as compared to C_s). We also see that the sensitivity to $\sigma_{\chi\chi}$ does become significantly worse as $m_\chi \rightarrow 4$ GeV. This is the critical m_χ below which the DM evaporations from the Sun is important.

4 Conclusion

We have studied the time evolution of DM number trapped inside the Sun with DM self-interaction considered. We have focused on the low m_χ range so that our analysis includes evaporation effects due to both DM-nuclei and DM-DM scatterings. The parameter region for the trapped DM inside the Sun to reach the equilibrium state is presented. We also found that the inclusion of DM self-interaction can increase the number of trapped DM and raise the evaporation mass scale. The parameter space on $\sigma_{\chi\chi} - \sigma_{\chi p}^{\text{SD(SI)}}$ plane for significant enhancement on trapped DM number ($R > 1$) is identified. The parameter space for $R > 1$ becomes larger for smaller m_χ . For $C_s < C_e$, the condition $R > 1$ leads to the suppression of neutrino flux, since the first term on the right hand side of eq. (2.16) is negative. We have proposed to study $\sigma_{\chi\chi}$ with the future IceCube-PINGU detector where the energy threshold can be lowered down to 1 GeV. We considered cascade and track events resulting from neutrino flux induced by DM annihilation channels $\chi\chi \rightarrow \nu\bar{\nu}$ and $\chi\chi \rightarrow \tau^+\tau^-$ inside the Sun. We found that cascade events always provide better sensitivity to $\sigma_{\chi\chi}$. The sensitivity to $\sigma_{\chi\chi}$ is also improved with a smaller DM annihilation cross section $\langle\sigma v\rangle$.

Acknowledgments

We thank S. Palomares-Ruiz for a very useful comment. CSC is supported by the National Center for Theoretical Sciences, Taiwan; FFL, GLL, and YHL are supported by Ministry of Science and Technology, Taiwan under Grant No. 102-2112-M-009-017.

A DM self-interaction induced evaporation

The derivation of DM self-interaction induced evaporation is similar to the usual nucleon induced evaporation [8–11]. One simply makes the parameter replacements

$$m_N \rightarrow m_\chi, \quad T_N \rightarrow T_\chi,$$

where T_χ is the DM temperature inside the Earth. The DM velocity distribution is approximated by Maxwell-Boltzmann distribution given by

$$f_\odot(w) = \frac{4}{\sqrt{\pi}} \left(\frac{m_\chi}{2T_\chi} \right)^{3/2} n_\chi w^2 \exp\left(-\frac{m_\chi w^2}{2T_\chi}\right),$$

where w is the DM velocity. The calculation of DM-DM scattering rate proceeds by choosing one of the DM as the incident particle and the other DM as one of the targets which satisfy Maxwell-Boltzmann distribution in their velocities. We then sum over the incident states

with Maxwell-Boltzmann distribution as well. Let the velocity of the incident DM be w and the velocity of the faster DM in the final state as v , respectively. Since we are considering the DM evaporation due to their self interactions, we have $v > w$.

It is essential to take note on the symmetry factor for identical particle scattering ($\chi\chi$ scattering) as compared to the DM-nucleus scattering studied before. We note that the faster DM with velocity v can be either one of the DM particles in the final state. This generates an extra factor of 2 relative to DM-nucleus scattering. On the other hand, due to identical particles in the initial state, a factor 1/2 must be applied as we sum over initial states according to thermal distributions. Hence the DM-DM differential scattering rate with the velocity transition $w \rightarrow v$ can be inferred from DM-nucleus scattering with suitable parameter replacements, which is given by

$$R^+(w \rightarrow v)dv = \frac{2}{\sqrt{\pi}} n_\chi \sigma_{\chi\chi} \frac{v}{w} e^{-\kappa^2(v^2-w^2)} \chi(\beta_-, \beta_+) dv, \quad (\text{A.1})$$

where we have summed up the target DM according to the thermal distribution f_\odot described above,

$$\beta_\pm = \pm \kappa w \quad \text{with} \quad \kappa = \sqrt{\frac{m_\chi}{2T_\chi}},$$

and

$$\chi(a, b) \equiv \int_a^b du e^{-u^2} = \frac{\sqrt{\pi}}{2} [\text{erf}(b) - \text{erf}(a)].$$

Therefore the DM-DM scattering rate with v greater than the escape velocity v_{esc} is given by the integral

$$\Omega_{v_{\text{esc}}}^+(w) = \int_{v_{\text{esc}}}^\infty R^+(w \rightarrow v') dv'. \quad (\text{A.2})$$

Carrying out the integral yields

$$\Omega_{v_{\text{esc}}}^+(w) = \frac{2}{\sqrt{\pi}} \frac{n_\chi \sigma_{\chi\chi}}{w} \frac{T_\chi}{m_\chi} \exp\left[\frac{m_\chi(v_{\text{esc}}^2 - w^2)}{2T_\chi}\right] \chi(\beta_-, \beta_+). \quad (\text{A.3})$$

To calculate the evaporation rate per unit volume at the position \vec{r} , we should sum up all possible states of the incident DM as follows:

$$\frac{dC_{se}}{dV} = \int_0^{v_{\text{esc}}} f_\odot(w) \Omega_{v_{\text{esc}}}^+(w) dw. \quad (\text{A.4})$$

The DM number density inside the Sun is determined by

$$n_\chi(r) = n_0 \exp\left(-\frac{m_\chi \phi(r)}{T_\chi}\right),$$

where n_0 is the density at the solar core, and $\phi(r)$ is the solar gravitational potential with respect to the core so that

$$\phi(r) = \int_0^r \frac{GM_\odot(r')}{r'^2} dr',$$

with G the Newton gravitational constant, $M_\odot(r) = 4\pi \int_0^r r'^2 \rho_\odot(r') dr'$ the solar mass enclosed within radius r , and $\rho_\odot(r)$ the solar density. Thus, the integration in eq. (A.4) can be performed

$$\frac{dC_{se}}{dV} = \frac{4}{\sqrt{\pi}} \sqrt{\frac{m_\chi}{2T_\chi}} \frac{n_0^2 \sigma_{\chi\chi}}{m_\chi} \exp\left[-\frac{2m_\chi \phi(r)}{T_\chi}\right] \exp\left[-\frac{E_{\text{esc}}(r)}{T_\chi}\right] \tilde{K}(m_\chi) \quad (\text{A.5})$$

where

$$\tilde{K}(m_\chi) = \sqrt{\frac{E_{\text{esc}}(r)T_\chi}{\pi}} \exp\left[-\frac{E_{\text{esc}}(r)}{T_\chi}\right] + \left(E_{\text{esc}}(r) - \frac{T_\chi}{2}\right) \text{erf}\left(\sqrt{\frac{E_{\text{esc}}(r)}{T_\chi}}\right), \quad (\text{A.6})$$

with $E_{\text{esc}}(r)$ the escape energy at the position r defined by

$$E_{\text{esc}}(r) = \frac{1}{2}m_\chi v_{\text{esc}}^2(r). \quad (\text{A.7})$$

The escape velocity $v_{\text{esc}}(r)$ is related to the gravitational potential by $v_{\text{esc}}(r) \equiv \sqrt{2[\phi(\infty) - \phi(r)]}$. Finally, the self-interaction induced evaporation rate can be evaluated through the following:

$$C_{se} = \frac{\int_\odot \frac{dC_{se}}{dV} d^3r}{\left(\int_\odot n_\chi(r) d^3r\right)^2}. \quad (\text{A.8})$$

References

- [1] G. Steigman, C.L. Sarazin, H. Quintana and J. Faulkner, *Dynamical interactions and astrophysical effects of stable heavy neutrinos*, *Astron. J.* **83** (1978) 1050 [INSPIRE].
- [2] D.N. Spergel and W.H. Press, *Effect of hypothetical, weakly interacting, massive particles on energy transport in the solar interior*, *Astrophys. J.* **294** (1985) 663 [INSPIRE].
- [3] W.H. Press and D.N. Spergel, *Capture by the sun of a galactic population of weakly interacting massive particles*, *Astrophys. J.* **296** (1985) 679 [INSPIRE].
- [4] J. Faulkner and R.L. Gilliland, *Weakly interacting, massive particles and the solar neutrino flux*, *Astrophys. J.* **299** (1985) 994 [INSPIRE].
- [5] K. Griest and D. Seckel, *Cosmic Asymmetry, Neutrinos and the Sun*, *Nucl. Phys. B* **283** (1987) 681 [Erratum *ibid.* **B 296** (1988) 1034] [INSPIRE].
- [6] G. Jungman, M. Kamionkowski and K. Griest, *Supersymmetric dark matter*, *Phys. Rept.* **267** (1996) 195 [hep-ph/9506380] [INSPIRE].
- [7] G. Bertone, D. Hooper and J. Silk, *Particle dark matter: Evidence, candidates and constraints*, *Phys. Rept.* **405** (2005) 279 [hep-ph/0404175] [INSPIRE].
- [8] A. Gould, *WIMP Distribution in and Evaporation From the Sun*, *Astrophys. J.* **321** (1987) 560 [INSPIRE].
- [9] R. Kappl and M.W. Winkler, *New Limits on Dark Matter from Super-Kamiokande*, *Nucl. Phys. B* **850** (2011) 505 [arXiv:1104.0679] [INSPIRE].
- [10] N. Bernal, J. Martín-Albo and S. Palomares-Ruiz, *A novel way of constraining WIMPs annihilations in the Sun: MeV neutrinos*, *JCAP* **08** (2013) 011 [arXiv:1208.0834] [INSPIRE].
- [11] G. Busoni, A. De Simone and W.-C. Huang, *On the Minimum Dark Matter Mass Testable by Neutrinos from the Sun*, *JCAP* **07** (2013) 010 [arXiv:1305.1817] [INSPIRE].
- [12] W.J.G. de Blok, *The Core-Cusp Problem*, *Adv. Astron.* **2010** (2010) 789293 [arXiv:0910.3538] [INSPIRE].
- [13] B. Moore, *Evidence against dissipationless dark matter from observations of galaxy haloes*, *Nature* **370** (1994) 629 [INSPIRE].
- [14] R.A. Flores and J.R. Primack, *Observational and theoretical constraints on singular dark matter halos*, *Astrophys. J.* **427** (1994) L1 [astro-ph/9402004] [INSPIRE].

- [15] J.F. Navarro, C.S. Frenk and S.D.M. White, *A Universal density profile from hierarchical clustering*, *Astrophys. J.* **490** (1997) 493 [[astro-ph/9611107](#)] [[INSPIRE](#)].
- [16] M.G. Walker and J. Penarrubia, *A Method for Measuring (Slopes of) the Mass Profiles of Dwarf Spheroidal Galaxies*, *Astrophys. J.* **742** (2011) 20 [[arXiv:1108.2404](#)] [[INSPIRE](#)].
- [17] S.-H. Oh, W.J.G. de Blok, E. Brinks, F. Walter and R.C. Kennicutt Jr., *Dark and luminous matter in THINGS dwarf galaxies*, *Astron. J.* **141** (2011) 193 [[arXiv:1011.0899](#)] [[INSPIRE](#)].
- [18] A.V. Maccio, S. Paduroiu, D. Anderhalden, A. Schneider and B. Moore, *Cores in warm dark matter haloes: a Catch 22 problem*, [arXiv:1202.1282](#) [[INSPIRE](#)].
- [19] D.N. Spergel and P.J. Steinhardt, *Observational evidence for selfinteracting cold dark matter*, *Phys. Rev. Lett.* **84** (2000) 3760 [[astro-ph/9909386](#)] [[INSPIRE](#)].
- [20] S.W. Randall, M. Markevitch, D. Clowe, A.H. Gonzalez and M. Bradac, *Constraints on the Self-Interaction Cross-Section of Dark Matter from Numerical Simulations of the Merging Galaxy Cluster 1E 0657-56*, *Astrophys. J.* **679** (2008) 1173 [[arXiv:0704.0261](#)] [[INSPIRE](#)].
- [21] M. Rocha, A.H.G. Peter, J.S. Bullock, M. Kaplinghat, S. Garrison-Kimmel et al., *Cosmological Simulations with Self-Interacting Dark Matter I: Constant Density Cores and Substructure*, *Mon. Not. Roy. Astron. Soc.* **430** (2013) 81 [[arXiv:1208.3025](#)] [[INSPIRE](#)].
- [22] A.H.G. Peter, M. Rocha, J.S. Bullock and M. Kaplinghat, *Cosmological Simulations with Self-Interacting Dark Matter II: Halo Shapes vs. Observations*, [arXiv:1208.3026](#) [[INSPIRE](#)].
- [23] J. Zavala, M. Vogelsberger and M.G. Walker, *Constraining Self-Interacting Dark Matter with the Milky Way's dwarf spheroidals*, *Mon. Not. Roy. Astron. Soc. Lett.* **431** (2013) L20 [[arXiv:1211.6426](#)] [[INSPIRE](#)].
- [24] I.F.M. Albuquerque, C. Pérez de Los Heros and D.S. Robertson, *Constraints on self interacting dark matter from IceCube results*, *JCAP* **02** (2014) 047 [[arXiv:1312.0797](#)] [[INSPIRE](#)].
- [25] ICECUBE collaboration, M.G. Aartsen et al., *Search for dark matter annihilations in the Sun with the 79-string IceCube detector*, *Phys. Rev. Lett.* **110** (2013) 131302 [[arXiv:1212.4097](#)] [[INSPIRE](#)].
- [26] A.R. Zentner, *High-Energy Neutrinos From Dark Matter Particle Self-Capture Within the Sun*, *Phys. Rev. D* **80** (2009) 063501 [[arXiv:0907.3448](#)] [[INSPIRE](#)].
- [27] P. Cushman, C. Galbiati, D.N. McKinsey, H. Robertson, T.M.P. Tait et al., *Working Group Report: WIMP Dark Matter Direct Detection*, [arXiv:1310.8327](#) [[INSPIRE](#)].
- [28] ICECUBE-PINGU collaboration, M.G. Aartsen et al., *Letter of Intent: The Precision IceCube Next Generation Upgrade (PINGU)*, [arXiv:1401.2046](#) [[INSPIRE](#)].
- [29] J.L. Feng, S. Ritz, J.J. Beatty, J. Buckley, D.F. Cowen et al., *Planning the Future of U.S. Particle Physics (Snowmass 2013): Chapter 4: Cosmic Frontier*, [arXiv:1401.6085](#) [[INSPIRE](#)].
- [30] M. Cirelli, G. Corcella, A. Hektor, G. Hutsi, M. Kadastik et al., *PPPC 4 DM ID: A Poor Particle Physicist Cookbook for Dark Matter Indirect Detection*, *JCAP* **03** (2011) 051 [Erratum *ibid.* **1210** (2012) E01] [[arXiv:1012.4515](#)] [[INSPIRE](#)].
- [31] C. Rott, J. Siegal-Gaskins and J.F. Beacom, *New Sensitivity to Solar WIMP Annihilation using Low-Energy Neutrinos*, *Phys. Rev. D* **88** (2013) 055005 [[arXiv:1208.0827](#)] [[INSPIRE](#)].
- [32] J.R. Ellis and R.A. Flores, *Realistic Predictions for the Detection of Supersymmetric Dark Matter*, *Nucl. Phys. B* **307** (1988) 883 [[INSPIRE](#)].
- [33] J. Engel and P. Vogel, *Spin dependent cross-sections of weakly interacting massive particles on nuclei*, *Phys. Rev. D* **40** (1989) 3132 [[INSPIRE](#)].
- [34] J. Engel, S. Pittel and P. Vogel, *Nuclear physics of dark matter detection*, *Int. J. Mod. Phys. E* **1** (1992) 1 [[INSPIRE](#)].

- [35] P.C. Divari, T.S. Kosmas, J.D. Vergados and L.D. Skouras, *Shell model calculations for light supersymmetric particle scattering off light nuclei*, *Phys. Rev. C* **61** (2000) 054612 [[INSPIRE](#)].
- [36] A. Gould, *Cosmological density of WIMPs from solar and terrestrial annihilations*, *Astrophys. J.* **388** (1992) 338 [[INSPIRE](#)].
- [37] COUPP collaboration, E. Behnke et al., *First Dark Matter Search Results from a 4-kg CF₃I Bubble Chamber Operated in a Deep Underground Site*, *Phys. Rev. D* **86** (2012) 052001 [[arXiv:1204.3094](#)] [[INSPIRE](#)].
- [38] M. Felizardo, T.A. Girard, T. Morlat, A.C. Fernandes, A.R. Ramos et al., *Final Analysis and Results of the Phase II SIMPLE Dark Matter Search*, *Phys. Rev. Lett.* **108** (2012) 201302 [[arXiv:1106.3014](#)] [[INSPIRE](#)].
- [39] LUX collaboration, D.S. Akerib et al., *First results from the LUX dark matter experiment at the Sanford Underground Research Facility*, *Phys. Rev. Lett.* **112** (2014) 091303 [[arXiv:1310.8214](#)] [[INSPIRE](#)].
- [40] M. Blennow, J. Edsjo and T. Ohlsson, *Neutrinos from WIMP annihilations using a full three-flavor Monte Carlo*, *JCAP* **01** (2008) 021 [[arXiv:0709.3898](#)] [[INSPIRE](#)].
- [41] R. Gandhi, C. Quigg, M.H. Reno and I. Sarcevic, *Ultrahigh-energy neutrino interactions*, *Astropart. Phys.* **5** (1996) 81 [[hep-ph/9512364](#)] [[INSPIRE](#)].
- [42] J. Hisano, K. Nakayama and M.J.S. Yang, *Upward muon signals at neutrino detectors as a probe of dark matter properties*, *Phys. Lett. B* **678** (2009) 101 [[arXiv:0905.2075](#)] [[INSPIRE](#)].
- [43] A.E. Erkoca, M.H. Reno and I. Sarcevic, *Muon Fluxes From Dark Matter Annihilation*, *Phys. Rev. D* **80** (2009) 043514 [[arXiv:0906.4364](#)] [[INSPIRE](#)].
- [44] J. Kumar, J.G. Learned, M. Sakai and S. Smith, *Dark Matter Detection With Electron Neutrinos in Liquid Scintillation Detectors*, *Phys. Rev. D* **84** (2011) 036007 [[arXiv:1103.3270](#)] [[INSPIRE](#)].
- [45] ICECUBE collaboration, M.G. Aartsen et al., *Measurement of the Atmospheric ν_e flux in IceCube*, *Phys. Rev. Lett.* **110** (2013) 151105 [[arXiv:1212.4760](#)] [[INSPIRE](#)].
- [46] M. Honda, T. Kajita, K. Kasahara, S. Midorikawa and T. Sanuki, *Calculation of atmospheric neutrino flux using the interaction model calibrated with atmospheric muon data*, *Phys. Rev. D* **75** (2007) 043006 [[astro-ph/0611418](#)] [[INSPIRE](#)].